PHYSICAL REVIEW A VOLUME 59, NUMBER 5 MAY 1999

Electron diffraction of trapped cluster ions

Mathias Maier-Borst, Douglas B. Cameron, Mordechai Rokni,* and Joel H. Parks†
Rowland Institute for Science, 100 Edwin H. Land Boulevard, Cambridge, Massachusetts 02142
(Received 1 December 1998)

A deeper understanding of the physics and chemistry of clusters has been constrained by the inability to observe experimentally the structure and structural variations for size selected clusters. We report here measurements of trapped ion electron diffraction, a technique that presents the possibility to directly observe the evolution of cluster structure with size and temperature. The results of electron diffraction from C_{60}^+ ions stored in a radio-frequency Paul trap are reported. [S1050-2947(99)50305-3]

PACS number(s): 36.40.Wa, 36.40.Mr, 61.14.−x, 61.48.+c

Direct measurement of the structure of mass-selected atomic clusters has presented such an exceedingly difficult challenge that studies of the physics and chemistry of gas-phase clusters [1] have proceeded for more than three decades without such a direct measurement. Cluster sources contribute to this difficulty since they produce beams with broad cluster size distributions of atomic number with uncertain internal energy distributions. Since an adequate cluster flux for diffraction measurements requires the full source output beam, the uncertainties in cluster size and internal energy prevent an unambiguous interpretation of electron-diffraction patterns [2–5]. This paper reports a technique that relies upon an rf Paul trap [6] to take advantage of the current cluster source technologies yet avoid the shortcomings of beam measurements. The rf Paul trap enables one to accumulate size selected clusters, collisionally relax the vibrational energy distribution, and store the clusters for an adequate time to perform electron-diffraction measurements. This can lead to a better experimentally controlled investigation of quantum-size effects and can provide the opportunity to probe the phase transformations for the transition region from molecular to bulk behavior.

The individual components of the experimental apparatus are schematically shown in Fig. 1. The rf trap, Faraday cup, and microchannel plate/phosphor screen detector (MCP) are mounted to maintain cylindrical symmetry around the electron beam axis. A charge-coupled-device (CCD) camera external to the UHV chamber images the diffraction pattern, which is in the form of Debye-Scherrer rings similar to powder diffraction as a result of the orientational and spatial disorder of the trapped cluster ions. The UHV chamber achieves a base pressure of $\sim 10^{-9}$ Torr and the pressure during diffraction measurements is $\leqslant 10^{-8}$ Torr.

The rf trap operates at 600 kHz with an end-cap electrode spacing of 1 cm. The diffraction *e* beam of ~0.5 mm diameter traverses the trap through 2-mm apertures in the grounded end-cap electrodes. Diffraction data are obtained at an *e*-beam energy of 40 keV and a beam current of ~400 nA. The diffraction volume and 2-mm end-cap aperture allow detection of scattered electrons with a maximum scattering angle of ±8.1°. For neutral beam diffraction measurements an effusive C_{60} beam emitted by a Knudsen oven traverses the trap at right angles to the *e* beam through 2-mm apertures in the ring electrode. For trapped C_{60}^+ measurements, ions are loaded into the trap by *in situ* ionization with a low-energy (~100 eV) electron gun and then vibrationally and translationally relaxed by a ~10-s exposure to He gas at a pressure of $\sim 10^{-4}$ Torr and a temperature of 300 K. After mass isolation of C_{60}^+ by resonance ejection of all other *m*/*z* ions, the C_{60}^+ ions were positioned at the trap operating point $q_z = 0.68$ (rf amplitude of $900 V_{0-p}$) during diffraction exposures. The *m*/*z* spectrum after the diffraction exposure is determined by resonantly ejecting the ions into the channeltron detector shown in Fig. 1.

A primary effort during the development of the trapped ion electron diffraction (TIED) technique was directed towards minimizing the background electron scattering. The small number of trapped cluster ions and their low-density results in such a low rate of elastic scattering relative to the incident electron-beam current ($\sim 10^{-9}$) that it makes the design and positioning of each component critically important. The lowest background electron scattering achieved was $i_{e\text{-back}}/i_{eb} = 1.6 \times 10^{-8}$, which was measured by counting the rate of single-electron events ($i_{e\text{-back}}$) detected by the microchannel plate detector (MCP) at low incident electron-beam current ($i_{eb} \sim 2$ nA) in the absence of cluster ions and at the chamber base pressure. This low level of background scattering was achieved by designing the Faraday cup as an electron trap with asymmetric entry and escape solid angles. In addition, the cup material was selected to maximize the conversion of high-energy electrons to x rays, which were then absorbed in the walls. The dominant noise contributions were from high-energy background electrons scattered from apertures, electrons reemerging from the Faraday cup, and scattering from residual gases in the UHV chamber.

Electron scattering from gas-phase molecules [7] is composed of (a) elastic scattering from individual atoms, (b) molecular terms arising from the interference of waves scattered by atoms separated by distances characteristic of the molecular structure, and (c) inelastic scattering characterized by the

*Permanent address: The Racah Institute of Physics, The Hebrew University, Jerusalem, Israel.
†Author to whom correspondence should be addressed. Electronic address: parks@rowland.org

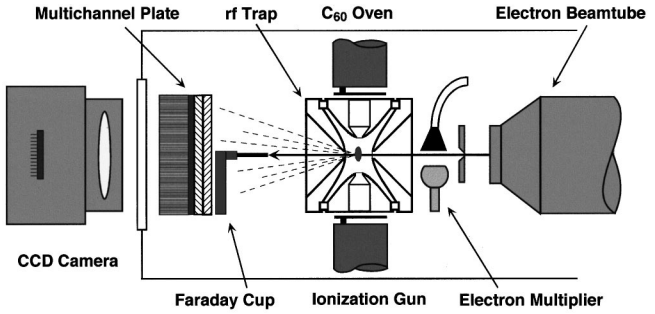

FIG. 1. The diffraction apparatus includes an rf trap, Faraday cup, and microchannel plate detector (MCP), and is structured to maintain a cylindrical symmetry around the electron-beam axis. The *e* beam passes through a trapped ion cloud producing scattered electrons, indicated by dashed lines. The primary beam enters the Faraday cup and scattered electrons strike an image quality MCP, producing a diffraction pattern on a phosphor screen. This screen is imaged by a scientific-grade CCD camera mounted external to the UHV chamber. The distance from the trapped ion cloud to the MCP is approximately 7.5 cm in these experiments. The channeltron electron multiplier detects ions ejected from the trap after a diffraction exposure.

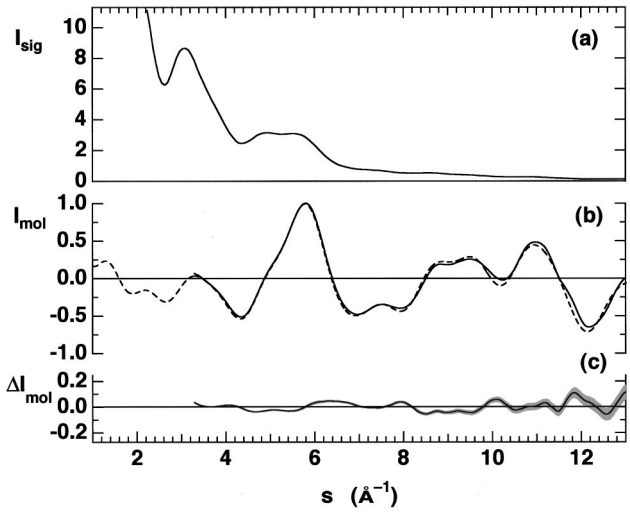

FIG. 2. Diffraction data for a neutral C_{60} beam. (a) The average diffraction intensity I_{sig} vs s (Å^{-1}) is obtained by averaging CCD pixels forming a circle around the *e*-beam axis. (b) Comparison of the experimental (solid curve) and theoretical (dashed curve) molecular scattering intensity I_{mol}. (c) The difference ΔI_{mol} is shown in with the uncertainty of $\pm 1\sigma$ (gray band) displayed at each data point.

electronic states. The total scattering intensity decreases as the fourth power of the momentum transfer $s = (4\pi/\lambda)\sin(\theta/2)$, where λ is the electron de Broglie wavelength (0.06 Å^{-1} for 40-keV electrons) and θ is the scattering angle.

Diffraction data were initially obtained from a neutral beam of C_{60} as it passed through the trap in the absence of rf voltage. The diffraction signal was first acquired for a period of time determined by the CCD pixel saturation, and then an electron background signal was obtained under identical conditions but with the C_{60} oven shutter closed. The measured background signal was uniformly distributed over the MCP detector surface. Using the C_{60} vapor pressure [8] at an oven temperature of ~800 K, the number of molecules in the volume defined by the intersection of the molecular and electron beams is estimated to be $\sim 5\times 10^5$. The electron background signal was subtracted from the diffraction signal pixel by pixel and the resulting CCD data array was averaged over 40 data sequences, each with an exposure time of 45 s. A total exposure time of 30 min at *e*-beam current of 410 nA was required to obtain data with high *S/N* over the range $3 \leqslant s$ (Å^{-1}) $\leqslant 13$. The plot of signal intensity I_{sig} vs s (Å^{-1}) shown in Fig. 2(a) is obtained by averaging the CCD data from pixels forming a circle around the electron-beam axis while discounting pixels shadowed by the Faraday cup.

The molecular signal [9] I_{mol}, which contains the structural information, was obtained from I_{sig} by subtracting a background arising from atomic elastic-scattering contributions and contributions from inelastic scattering. This was accomplished using a trial and error method similar to that described in Ref. [10], which relies upon the expected zero crossings of the molecular diffraction term, calculated by assuming a given molecular structure. In Fig. 2(b) the experimental molecular diffraction signal I_{mol} is compared with the theoretical prediction. The theoretical curve has been calculated using vibrational amplitude parameters derived from the C_{60} gas-phase diffraction data of Hedberg *et al.* [11], and it has also been smoothed to account for the finite electron-beam diameter of ~0.5 mm. Figure 2(c) displays the difference ΔI_{mol} between experiment and theory. The gray band superimposed on ΔI_{mol} represents the standard deviation at each data point. Our C_{60}-beam experimental data closely reproduce the Hedberg *et al.* [11] results. This agreement was essential for our evaluation of the data reduction analysis and the constraints imposed by electron background scattering and detector saturation limits.

The possible effects of the trap rf field on the scattered electrons was studied by comparing diffraction data produced by a neutral C_{60} beam passing through trap center with

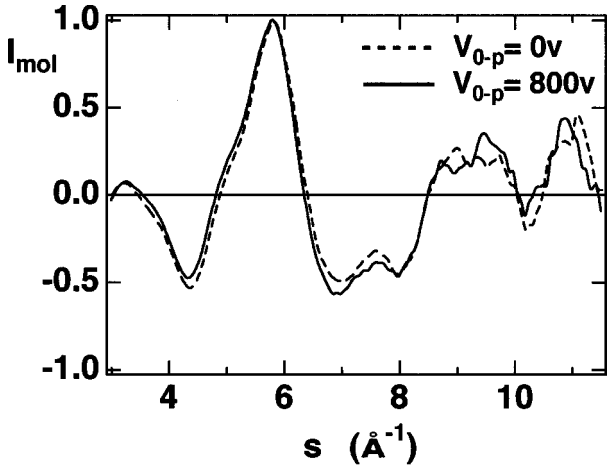

FIG. 3. Comparison of molecular diffraction data produced by *e*-beam scattering from a neutral C_{60} beam in the presence of the rf field (solid curve) with that obtained with the rf field off (dashed curve).

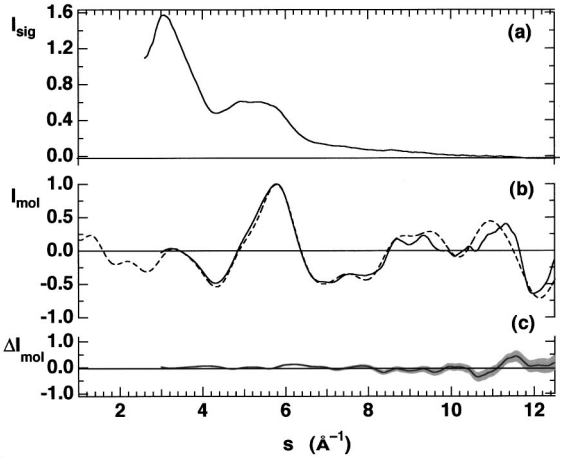

FIG. 4. Diffraction data for trapped C_{60}^+ ions. (a) The average diffraction intensity $I_{\rm sig}$ vs s (Å^{-1}), is obtained by averaging CCD pixels forming a circle around the e-beam axis. (b) Comparison of the experimental (solid curve) and theoretical (dashed curve) molecular scattering intensity $I_{\rm mol}$. (c) The difference $\Delta I_{\rm mol}$ is shown with the uncertainty of $\pm 1\sigma$ (gray band) displayed at each data point.

the rf field on with that obtained with the rf field off. The data comparison shown in Fig. 3 indicates that rf trap voltages up to $800V_{0-p}$ produce no appreciable effect on the detected diffraction pattern. This is consistent with our estimates of the perturbations of the scattering angle and of the electron energy by the rf field. However, measurement of the background electron-scattering intensity did indicate a slight increase in the presence of the rf field. The degree to which this might constrain the applicable rf voltage amplitude will depend on the diffracting species.

Diffraction data were obtained from trapped C_{60}^+ during an experimental run composed of repeated trap loadings as described above. An average of $\sim 2\times 10^4$ C_{60}^+ ions were stored initially for each diffraction exposure. The background electron-scattering signal was obtained by exposing an empty trap for an identical exposure time. The plot of average diffraction intensity $I_{\rm sig}$ vs s (Å^{-1}) shown in Fig. 4(a) was obtained by averaging over 360 data sequences with an exposure time of 45 s each. A total exposure time of 4.5 h at an e-beam current of 400 nA was required to obtain $\sim 10 \geqslant S/N \geqslant 2$ over the range $3 \leqslant s$ (Å^{-1}) $\leqslant 13$, respectively. The total experimental run time, including the electron background measurement and the trap loading/ejection sequences, was 12 h.

The trapped C_{60}^+-ion molecular diffraction intensity $I_{\rm mol}$ is compared with theoretical calculations for neutral C_{60} in Fig. 4(b). Figure 4(c) displays the difference $\Delta I_{\rm mol}$, and the superimposed gray band represents the standard deviation at each data point. The increased deviation between data and theory as s increases is the result of weaker scattering at larger angles compounded by a less reliable fitting of the background scattering for large s values. Although the S/N is reduced by a factor of ~ 8 relative to the neutral beam data, the diffraction pattern is clearly consistent with that of neutral C_{60}. This S/N level precludes a more careful analysis to determine the presence of Jahn-Teller distortions predicted [12] for C_{60}^+ ions.

Inelastic electron-scattering channels were also studied by exposing the trapped ions for 5 min to a 100-nA beam of 40-keV electrons used for the diffraction experiments. Exposure to the 40-keV beam resulted in only a slight decrease in the number of C_{60}^+ ions, in marked contrast to the large conversion of C_{60}^+ to fragmentation products C_{60-2n}^+ and multiply charged ions C_{60}^{z+} observed [13] for low-energy e beams (100 eV). The dominant inelastic scattering channel we observed at these high energies was the production of multiply charged ions; however, no fragmentation was observed for any charge state. This is consistent with previous measurements of the excitation of gas-phase C_{60} by high-energy electrons [14] and photons [15], which identified an autoionization channel via the surface plasmon excitation near 20 eV as the dominant inelastic process. The cross section for the loss of a C_{60}^+ ion by inelastic processes is estimated to be $\sigma \sim 2\times 10^{-18}$ cm^2, which is comparable to measurements [16] of the second ionization cross section of Li^+ by 25-keV electrons. During the 45-s exposure time of the diffraction measurements, all multicharged ions produced by inelastic scattering were unstable at the trap operating point of $q_z = 0.68$ and could not contribute to the diffraction data.

This Rapid Communication has introduced an experimental method of trapped ion electron diffraction and has successfully demonstrated the technique by measuring diffraction patterns from $\sim 2\times 10^4$ C_{60}^+ ions stored within an rf Paul trap. Obtaining diffraction from trapped C_{60}^+ ions was an exceptionally severe test of the method since the weak scattering cross section required long exposure times (4.5 h) to achieve diffraction patterns with $\sim 10 \geqslant S/N \geqslant 2$ over the range of $3 \leqslant s$ (Å^{-1}) $\leqslant 13$. However, these experiments demonstrated that the experimental apparatus is capable of providing reproducible results over long run durations.

The inelastic scattering channels will always be an important consideration. The dominant inelastic channel in these experiments was ionization and not fragmentation of the trapped ion. This may be unique to C_{60}^+ ions and the inelastic scattering will have to be measured for each species studied.

The diffraction experiments with C_{60}^+ ions provide information to evaluate the possibilities for more interesting clusters and molecular-ion species. For example, we are currently considering a study of the structure and phase transitions of gold clusters [17], which have recently been the subject of extensive calculations [18–20]. Diffraction studies of alloyed clusters (e.g., Au_nSi_m) could provide an opportunity to observe the competition between atomic segregation and stoichiometric mixtures as a function of size and temperature. Finally, it may be possible to extend TIED to biopolymers, which suggests that measurements related to protein conformation dynamics might be considered.

This research was fully supported by The Rowland Institute for Science. We would like to thank Tom Tyrie and Peg Charpentier of Kimball Physics Inc. for helping to optimize the electron gun operation.

[1] *Clusters of Atoms and Molecules*, edited by H. Haberland, Springer Series in Chemical Physics, Vol. 52 (Springer-Verlag, Berlin, 1994).

[2] B. G. De Boer and G. D. Stein, Surf. Sci. **106**, 84 (1981); A. Yokozeki and G. Stein, J. Appl. Phys. **49**, 2224 (1978).

[3] J. Farges, M. F. Feraudy, B. Raoult, and G. Torchet, Surf. Sci. **106**, 95 (1981); J. Farges, B. Raoult, and G. Torchet, J. Chem. Phys. **59**, 3454 (1973).

[4] J. W. Hovick and L. S. Bartell, J. Phys. Chem. B **102**, 534 (1998); L. S. Bartell, Chem. Rev. **86**, 491 (1986).

[5] D. Reinhard, B. D. Hall, D. Ugarte, and R. Monot, Phys. Rev. B **58**, 4917 (1998); D. Reinhard, B. D. Hall, P. Berthoud, S. Valkealahti, and R. Monot, *ibid.* **55**, 7868 (1997).

[6] J. H. Parks, S. Pollack, and W. Hill, J. Chem. Phys. **101**, 6666 (1994); J. H. Parks and A. Szöke, *ibid.* **103**, 1422 (1995).

[7] *Stereochemical Applications of Gas-Phase Electron Diffraction*, edited by I. Hargittai and M. Hargittai (VCH, New York, 1988).

[8] J. Abrefah, D. R. Olander, M. Balooch, and W. J. Siekhaus, Appl. Phys. Lett. **60**, 1313 (1992); K. Mathews *et al.*, J. Phys. Chem. **96**, 3566 (1992); V. Piacente, G. Gigli, P. Scardala, A. Giustini, and D. Ferro, *ibid.* **99**, 14 052 (1995).

[9] The molecular scattering intensity I_{mol} is defined here as $I_{\mathrm{mol}}=s^4\{I_{\mathrm{sig}}-I_{\mathrm{back}}\}$ to extract the rapid s dependence from the diffraction data analysis, where I_{sig} is the average diffraction signal intensity and I_{back} is the background diffraction signal. We note that $I_{\mathrm{mol}}=sM(s)$ for comparison with analyses that express the molecular diffraction in terms of the modified molecular scattering intensity $sM(s)$.

[10] P. D'Antonio, C. George, A. H. Lowrey, and J. Karle, J. Chem. Phys. **55**, 1071 (1971).

[11] K. Hedberg *et al.*, Science **254**, 410 (1991).

[12] C. C. Chancey and M. C. O'Brien, *The Jahn-Teller Effect in C_{60} and Other Icosahedral Complexes* (Princeton University Press, Princeton, 1997).

[13] D. B. Cameron and J. H. Parks, Chem. Phys. Lett. **272**, 18 (1997).

[14] A. W. Burose, T. Dresch, and A. M. Ding, in *Electronic Properties of Fullerenes*, edited by H. Kuzmany, J. Fink, M. Mehring, and S. Roth (Springer-Verlag, Berlin, 1993); J. W. Keller and M. A. Coplan, Chem. Phys. Lett. **193**, 89 (1992).

[15] T. Drewello, W. Krätschmer, M. Fieber-Erdmann, and A. Ding, in *Electronic Properties of Fullerenes* (Ref. [14]); H. Steger, J. De Vries, B. Kamke, and W. Kamke, Chem. Phys. Lett. **194**, 452 (1992); I. V. Hertel *et al.*, Phys. Rev. Lett. **68**, 784 (1992).

[16] B. Peart and K. T. Dolder, J. Phys. B **2**, 1169 (1969).

[17] T. G. Schaaff *et al.*, J. Phys. Chem. B **101**, 7885 (1997).

[18] C. L. Cleveland *et al.*, Phys. Rev. Lett. **79**, 1873 (1997).

[19] I. L. Garzón *et al.*, Phys. Rev. Lett. **81**, 1600 (1998).

[20] C. L. Cleveland, W. D. Luedtke, and U. Landman, Phys. Rev. Lett. **81**, 2036 (1998).